

# Development of Refractive Error Detection Wavefront Technology based on Quadriwave Lateral Shearing Interferometry (QWLSI): A Comprehensive Study

Reynaldo Jr. T. Belen, Precious Reyna G. Casballido, Era May Crisostomo, Joshua Rei S. Galdonez,  
Joseph Francis B. Gambol, Philip Joshua C. Navea  
*Electronics Engineering Department, College of Engineering  
Technological University of the Philippines - Manila  
Ayala Boulevard, Ermita, Manila, Philippines*

Email: [francisjoseph1529@gmail.com](mailto:francisjoseph1529@gmail.com)

## I. INTRODUCTION

Wavefront technology has revolutionized a variety of industries, including astronomy and ophthalmology. It is a crucial improvement in the study and manipulation of optical phenomena. Adaptive optics is a brilliant technique that early astronomers used to sharpen blurry images captured by ground-based telescopes. This invention was crucial to the ground-breaking finding of a supermassive object at the center of our galaxy. [1] In the 1900s, an astronomer named Johannes Hartmann invented a new way to measure how well telescope mirrors and lenses focused light. His method involved shining light through a special metal plate with holes in it and then analyzing the light patterns to reveal any imperfections in the mirrors or lenses. [2] From its early beginnings in the 19th century to the sophisticated techniques of today, wavefront technology has continually evolved to unlock unprecedented insights into the behavior of light. Among the myriad applications, one notable advancement is the rising wavefront imaging technique called Quadriwave Lateral Shearing Interferometry (QWLSI), a cutting-edge technique that has significantly contributed to the field of optical diagnostics. [3]

Interferometry has become an effective method for revealing secrets hidden in a wavefront. Combining two or more light beams results in an interference pattern that encodes information about the relative phases of the waves. Robert Hooke first presented this idea in the 17th century. With the ability to quantify even the smallest wavefront aberrations, interferometry is revolutionizing a number of industries, most notably refractive error detection. [4] The concept behind QWLSI builds upon Lateral Shearing Interferometry (LSI), a technique introduced in 1971. One of the characteristics of the LSI interferometer is its ability to duplicate the testing wavefront twice with equal amplitudes and mutual displacement. It is surprising that LSI interferometers are not employed more frequently despite these advantageous characteristics. This is mostly because there are certain ambiguous features to the signal processing on this type of sheared data. [5] With that, QWLSI emerged around the year 2000, addressing the limitations of LSI. QWLSI is used to precisely and accurately evaluate wavefront. QWLSI employs a diffractive grating to create four laterally shifted and tilted replicas of the wavefront.

This allows for the simultaneous measurement of wavefront derivatives along four directions, providing a more comprehensive analysis. [6]

Vision impairment arises when an eye-related issue impacts the functioning of the visual system and its ability to perceive visual stimuli. It is inevitable that at some point in their lives, individuals will encounter at least one eye condition necessitating proper treatment and care. Vision impairment poses significant challenges for individuals throughout their lives, but timely access to high-quality eye care can help alleviate many of these challenges. Eye conditions like cataracts or refractive errors, which have the potential to cause vision impairment and blindness, are prioritized in eye care strategies for their considerable impact. Refractive errors, cataracts, diabetic retinopathy, glaucoma, and age-related macular degeneration stand as the primary contributors to vision impairment and blindness on a global scale. Uncorrected refractive errors continue to be a prominent cause of vision impairment across all age groups and countries worldwide. Therefore, it is imperative to develop strategic approaches to tackle eye conditions in order to prevent vision impairment. [7].

## II. THEORETICAL BACKGROUND

### A. Aberrometry

Wavefront sensing (aberrometry) emerged from a lab application to a universal ophthalmological tool when Bille and coworkers were the first to measure the ocular wavefront aberration in 1978 [8]. The Technique of measurement of aberrations in the eye (imperfections of the optical system) is called aberrometry [11]. Since then, The ocular wave deformation comprehensively reflects the optical properties of the eye. This is important clinically, because with conventional techniques only spherical and cylindrical error (so-called lower order aberrations) can be measured. However, there are optical aberrations (so-called higher order aberrations) that could neither be measured with conventional techniques nor be corrected with spectacles.

### B. Microlens Array (MLA)

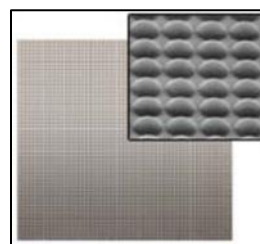


Figure 2: Microlens Array  
(adapted from <https://www.thorlabs.com/>)

Microlenses are discrete or array- based spheres, aspheres and other optics being used for focusing light inside fibers for optical networking or vision system. In general, microlenses have a diameter between 10μm–5mm and a curvature radius of 0.25—2.5mm. Microlens arrays also known as MLAs consists of series of miniaturized lenses

either squarely or hexagonally packed which are in a form of certain arrangement [13]. These microlenses, whose surface profiles can be convex or concave depending on its applications, are normally cylindrical, square or hemispherical in shape. Therefore, when a single light beam is incident to a microlens array, thousands and sometimes millions of tiny light spots are generated at the focal plane of the microlens arrays, depending on the size of the microlenses. Square microlens, which is usually 10mm x 10mm, are usually used in wavefront sensors [14].

### The Diffraction Grating

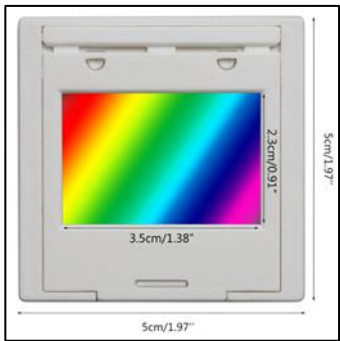


Figure 2: 1-Dimension Diffraction Grating (Adapted from: www.shopee.com)

A diffraction grating is a collection of reflecting (or transmitting) elements separated by a distance (known as slits) comparable to the wavelength of light under study. It may be visualized as a collection of diffracting elements in a material, such as a pattern of transparent slits (or apertures) in an opaque screen or detector. Upon diffraction, an incident electromagnetic wave travelling on a grating will have its electric field amplitude, or phase, or both, modified in a predictable manner, due to the periodic variation when passing through with the effects of refractive index in the region near the surface of the grating [9]. The manufacturer Ivzosheng used PET/Plastic material for its 100lines/mm diffraction grating with grating size equal to 38x36mm and thickness equal to 2mm. That supports a wavelength up to 200nm-10000nm [10].

### C. Wavefront Technologies - Interferometry

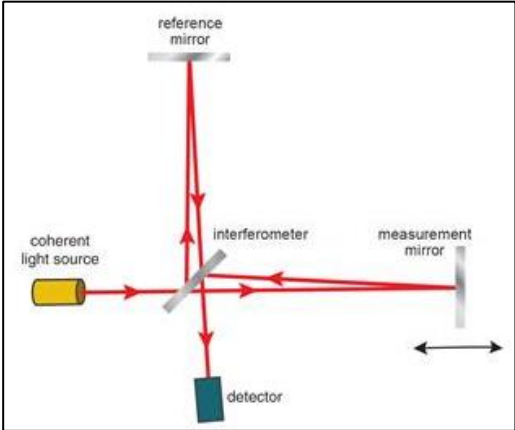


Figure 3: Michelson interferometer (adapted from [19])

Optical interferometers are instruments that creates an interferogram that use interference of two or more superimposed light beams in its imaging system [17]. These

are one of the most common optical tools, and are used for precision measurements, surface diagnostics, astrophysics, seismology, quantum information, etc. The shearing interferometry is the most used technique in many configurations of optical interferometers. The recorded interferometry is between the incoming wavefront (measurement mirror) and its displaced replica (reference mirror). One method of modification the set-up is through phase-shifting by means of “lateral shear”, if the input is shifted by two lens that creates the wavefront. The object (e.g., the retina) is illuminated with a single beam of coherent light. In the simplest case scenario, a grating is placed in front of the object (e.g. the eye) to provide two sheared images of the object. The object is then imaged onto a CCD Array, Detector or a camera. A shearing device in the imaging system results in two superimposed images in which it is interpreted as one image as the eye can comprehend. Therefore, the wavefront can be analyzed between the grating and the camera, over a couple of millimeters. any pixel in the sensor device usually a camera detector receives light from two points on the object surface and the phase changes at the pixel then depend directly on the relative displacement of the two points. the sheared wavefronts can be generated by a grating mounted on a translation stage, a phase-shifted casing. The interference pattern also known as Spot Diagram specifically the Interferogram is generated in the overlap area [12].

### D. Quadriwave Lateral Shearing Interferometry Principle

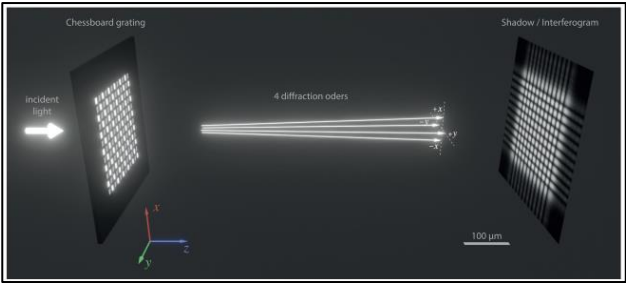


Figure 4: The simplest setup of QWLSI consisting of Information light signal, diffraction gratings, and a detector for the interferogram (adapted from: [16])

Quadriwave Lateral Shearing Interferometry (QWLSI) also known as QLSI, is a quantitative phase imaging technique based on the use of a wavefront analyzer composed of two simple elements: a regular camera and a 2-dimensional diffraction grating, separated by millimetric distance from each other creating the lateral shearing. Once illuminated into the diffraction grating (usually called a modified Hartmann mask, MHM) creates an interferogram on the camera sensor that can be processed to retrieve both the intensity and the wavefront profiles or equivalently the phase of an incoming light beam [15]. The interferogram created by the interference of the four replicas is constituted with bright spots disposed according a Cartesian geometry as it is shown on Figure and which undergoes deformations if the incident wave-front is aberrant [18].

### E. Aberrations

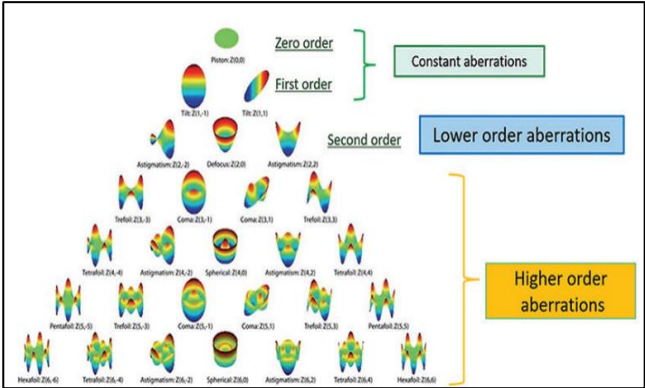


Figure 5: Zernike Pyramid (adapted from: [12])

Asphericity, denoted as Q, is the representation of change in the curvature of an ellipsoid surface from the center toward the edges. The human eye is prone to flaws in the optical system and has several ocular aberrations. Ocular aberrations are deviations of the wavefront from the reference ‘aberration-free’ wavefront. These flaws can influence their measurements such as pupil size, tear film stability, lid position, accommodation and fixational eye movements. Symptoms of aberration include glare, halos, starbursts and ghosting [11].

Monochromatic aberrations is a type of that occur due to the geometry of the lens and corneal curvatures and their respective refractive indices. Based on Zernike’s polynomials, these can be classified as lower-order aberrations (LOA) and higher-order aberrations (HOA). LOA are further classified as zero-order, first-order, and second-order aberrations. HOA are those above second-order aberrations [11].

Zero-order (Piston) and first-order (tilt) aberrations are called constant aberrations. These are present in all optical systems and they are visually non-significant [11].

Second-order aberrations are lower-order aberrations, which consist of defocus and astigmatism. Defocus comprises both myopia (near-sightedness) and hyperopia(far-sightedness), that is, spherical defocus. A positive defocus is called and a negative defocus is called hyperopia. Astigmatism comprises horizontal and vertical astigmatism, that is, x- and y-astigmatism, respectively. These aberrations can be easily alleviated by prescribing spectacles, contact lenses or by refractive surgery [11].

Higher-order aberrations include coma, spherical aberration, secondary astigmatism, trefoil, and many more. Out of these, coma and spherical aberration are most likely to affect visual performance as they result in a distorted wavefront. These aberrations can negatively affect the vision of apparently healthy eyes and cannot be corrected using spectacles or contact lenses [11].

### III. OBJECTIVES

1. To design and develop a Quadriwave Lateral Shearing Interferometry (QWLSI) wavefront technology that will perform refractive error detection comprising of both higher-order aberrations and lower-order aberrations.
2. To compare and evaluate the results obtained with the device against traditional method of testing.

### IV. METHODOLOGY

This section explains the construction of the wavefront sensor using the Quadriwave Lateral Shearing Interferometry Principle (QWLSI)

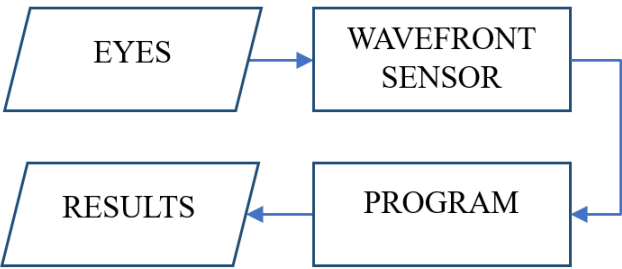


Figure 6. General Block Diagram

Figure 6 shows the general block diagram of the hardware. The wavefront sensor is able to generate a raw image of the wavefront of the user’s eye. It will be then utilized by a program in charge to obtain the desired output. The raw image from the sensor produces information that can be used to determine the LOA and HOA.

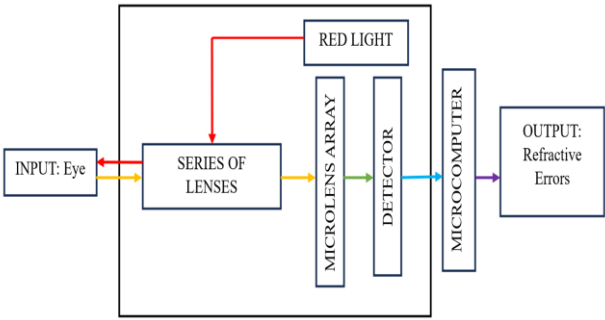


Figure 7. Wavefront Sensor Diagram

The process of refractive error detection using this sensor involves activating a red light of 650 to 700nm wavelength, which is directed into the eye’s retina using a system of lenses comprising of beamsplitters and plane mirrors. At this point, the type of aberration can be determined and needs to be captured. The wavefront will be reflected spontaneously and will pass through an M9\*5 collimating lens, then parallelized again by a second beam splitter with a 10x10mm area. This light will then pass through a 10x10mm 2D diffraction grating, creating an image of the wavefront. The 2D diffraction grating is created by orthogonally stacking two 1D diffraction gratings, resulting in a modulo 2-pi phase addition of the respective diffraction gratings. The pattern has its most intense value at 2-pi and the least intense value at 0 (Anand, 2015). The lateral shearing displacement of the two gratings is around 2-3mm [20]. This wavefront, a collection of light from the eye’s retina with the achromatic appearance of the source light, will be captured by the Detector. This image will be transmitted to the microprocessor for computation.

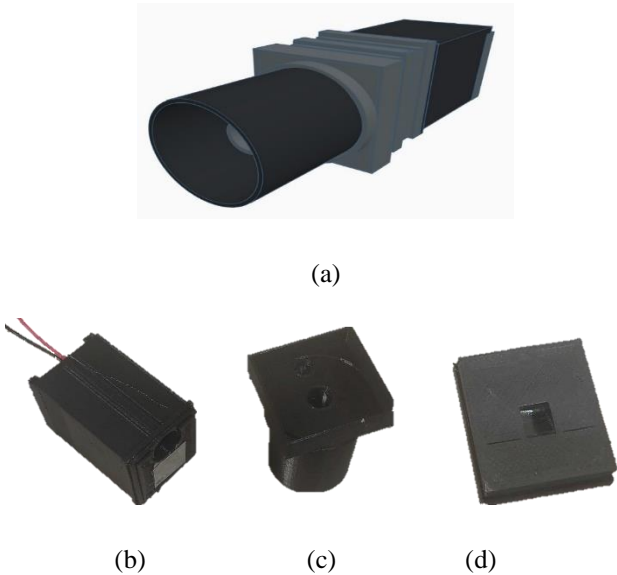


Figure 8. Construction of Wavefront Sensor (a) Overall Appearance using 3D Software (b) Detector (c) Collimating Case (d) Casing of the Series of Lenses

Figure 8 shows the construction of the wavefront sensor. The base, as shown in Figure 5.a, is composed of the screen where the results can be seen, power bank as the power source, circuit for the LED, switch to turn on and off the prototype and the microcontroller. In figure 5.b shows the top part of the prototype, it is designed like a telescope. It has an eyecup where the users can peek for them to be examined. While in Figure 5.c shows what’s inside the top part, it is composed of the camera and its ribbon, which is connected to the microcontroller, the collimating lens and microlens array.



V. RESULTS

This section presents the wavefront sensor using QWLSI principle, its specifications and the sample raw image acquired.

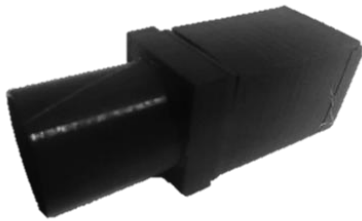


Figure 9. QWLSI Wavefront Sensor

Figure 6 shows the final design of the prototype. The 3D printed case is supported by a modified bolt and nut that can be adjusted depending on the height of the user. The cylindrical cup is where the user’s eye peeks in. and once it is captured, it will be done by software computations.

Table 1. Confusion Matrix Analysis of the Wavefront Sensor and Clinical Results for Left Eye of SPH measurement

Measure	Calculated Values
Accuracy	0.16
Misclassification Rate	0.84

Table 2. Confusion Matrix Analysis of the Wavefront Sensor and Clinical Results for Left Eye of CYL measurement

Measure	Calculated Values
Accuracy	0.6
Misclassification Rate	0.4

Table 3. Confusion Matrix Analysis of the Wavefront Sensor and Clinical Results for Left Eye of AX measurement

Measure	Calculated Values
Accuracy	0.32
Misclassification Rate	0.68

Table 4. Confusion Matrix Analysis of the Wavefront Sensor and Clinical Results for Right Eye of SPH measurement

Measure	Calculated Values
Accuracy	0.2
Misclassification Rate	0.8

Table 5. Confusion Matrix Analysis of the Wavefront Sensor and Clinical Results for Right Eye of CYL measurement

Measure	Calculated Values
Accuracy	0.64
Misclassification Rate	0.36

Table 6. Confusion Matrix Analysis of the Wavefront Sensor and Clinical Results for Right Eye of AX measurement

Measure	Calculated Values
Accuracy	0.52
Misclassification Rate	0.48

In table 6, the specifications of the wavefront sensor and the images captured by the wavefront sensor.

Table 6. Overall Specifications of the Wavefront Sensor

SPECIFICATIONS OF THE WAVEFRONT SENSOR	
Parameter	Value
Array Size and Type	10x10mm, square grid
Microlens used	2-Dimensional Diffraction Grating
Lens Pitch	100-150µm
Pixel Size, Optical Size	1.12 µm x 1.12 µm, ¼”
Focal Length	3.04mm
Camera Resolution	8 Megapixels, 3280 × 2464 pixels
Light Wavelength	650-700nm
Operating Hours	24-30hrs
Input	2 wire line for light, Ribbon cable for detector

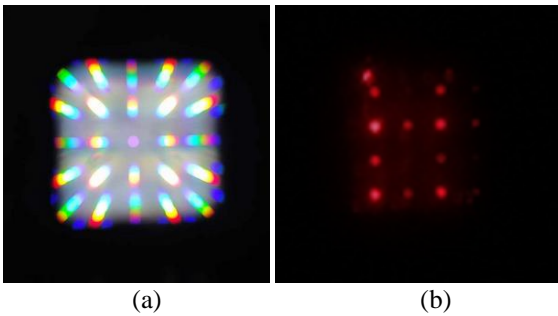


Figure 10. Light passes through the Microlens Array (a) White Light (b) Red Light

Figure 10 shows the sample raw images that was obtained from the wavefront sensor. It is noticeable that each image has differences. The raw image contains spots. Each image has different level of brightness in their own spot. Also, the number of spots, Therefore, each image profile contains different information. Once processed using different algorithms, data from each image will be very helpful in obtaining the desired output.

VI. CONCLUSION

Wavefront technology is very essential in today’s generation for it has numerous applications. Wavefront sensing using Quadriwave Lateral Shearing Interferometry (QWLSI) principle is one of it. The wavefront sensor is composed of a Detector such as a CMOS Pi Camera, collimating lens, visual stimulus and microlens array specifically the 2D Diffraction Grating. When the light enters the human eye, it is reflected and will be captured by the wavefront sensor. From the raw data obtained by the sensor, it is can be processed and interpreted by a software.

Each spot in the raw image contains relevant information that is useful in detecting the higher and lower order aberrations. With the use of this sensor, early detection of the aberrations in the eyes and the immediate correction using contact lenses, eyeglasses, or refractive surgeries will prevent further complications that may occur. However, there can be further improvements here, by using a clinical type of lens instead to the commercially used one and improving the QWLSI Algorithm for the microprocessor.

REFERENCES

[1] Hampson KM;Turcotte R;Miller DT;Kurokawa K;Males JR;Ji N;Booth MJ;, “Adaptive optics for high-resolution imaging,” Nature reviews. Methods primers, <https://pubmed.ncbi.nlm.nih.gov/35252878/> (accessed Mar. 13, 2024).

[2] E. Weinlander, “Wavefront testing,” EyeWiki,

- [https://eyewiki.aao.org/Wavefront\\_Testing](https://eyewiki.aao.org/Wavefront_Testing) (accessed Mar. 13, 2024).
- [3] G. Baffou, "Wavefront microscopy using Quadriwave lateral shearing interferometry: From bioimaging to Nanophotonics," *ACS Photonics*, vol. 10, no. 2, pp. 322–339, Jan. 2023. doi:10.1021/acsp Photonics.2c01238
- [4] P. Hariharan, *Basics of Interferometry*, 2nd ed. Elsevier Inc., 2007.
- [5] M. Servin, M. Cywiak, and A. Davila, "Extreme shearing interferometry: Theoretical limits with practical consequences," *Optics Express*, vol. 15, no. 26, p. 17805, 2007. doi:10.1364/oe.15.017805
- [6] S. Velghe et al., "Advanced wave-front sensing by Quadri-wave lateral shearing interferometry," *Interferometry XIII: Techniques and Analysis*, Aug. 2006. doi:10.1117/12.681533
- [7] "Vision Impairment and blindness," World Health Organization, <https://www.who.int/news-room/fact-sheets/detail/blindness-and-visual-impairment> (accessed Mar. 13, 2024).
- [8] Spaeth, G. L. (1982). *Ophthalmic surgery, principles and practice*. <http://ci.nii.ac.jp/ncid/BA07821701> (accessed Mar. 13, 2024).
- [9] Palmer, C., & Loewen, E. G. (2005). *Diffraction grating handbook*. <https://diverdi.colostate.edu/C431/experiments/time%20domain%20fluorescence/diffraction%20gratings/Richardson%20Gratings%20Handbook.pdf>(accessed Mar. 13, 2024).
- [10] Diffraction Grating PET Plastic Optical Grate Teaching Demonstrator | - AliExpress. (n.d.). [https://www.aliexpress.com/item/1005006143364610.html?src=google&aff\\_fcid=19fb78b47692423a9fa247ba26ee6a75-1710236729729-01009-UnaMJZVf&aff\\_fsk=UnaMJZVf&aff\\_platform=aaf&sk=UnaMJZVf&aff\\_trace\\_key=19fb78b47692423a9fa247ba26ee6a75-1710236729729-01009-UnaMJZVf&terminal\\_id=1802b3c39b6443478bd8677514440052&afSmartRedirect=y](https://www.aliexpress.com/item/1005006143364610.html?src=google&aff_fcid=19fb78b47692423a9fa247ba26ee6a75-1710236729729-01009-UnaMJZVf&aff_fsk=UnaMJZVf&aff_platform=aaf&sk=UnaMJZVf&aff_trace_key=19fb78b47692423a9fa247ba26ee6a75-1710236729729-01009-UnaMJZVf&terminal_id=1802b3c39b6443478bd8677514440052&afSmartRedirect=y) (accessed Mar. 13, 2024).
- [11] Christy, J. S., & Parab, A. (2023). Aberrometry in ophthalmology and its applications in cataract surgery. *tnoa Journal of Ophthalmic Science and Research*, 61(1), 32-40. (accessed Mar. 13, 2024).
- [12] Vacalebri, M., Frison, R., Corsaro, C., Neri, F., Conoci, S., Anastasi, E., ... & Fazio, E. (2022). Advanced optical wavefront technologies to improve patient quality of vision and meet clinical requests. *Polymers*, 14(23), 5321. (accessed Mar. 13, 2024).
- [13] SEONG, L. C. (2008). *Micro Lens Array Fabrication Technique and its Application in Surface Nanopatterning*. (accessed Mar. 13, 2024).
- [14] Atas, M. C. D., Landicho, L. M. T., Lobo, A. D., Orubia, C. J. L., Silverio, A. C. O., Aquino, A. U., Amado, T. M., Puno, J. C. V., Quijano, J. F. C., & Arago, N. M. (2019). Development of Wavefront Sensor using Shack-Hartmann Principle. In 2019 IEEE 11th International Conference on Humanoid, Nanotechnology, Information Technology, Communication and Control, Environment, and Management (HNICEM ). 2019 IEEE 11th International Conference on Humanoid, Nanotechnology, Information Technology, Communication and Control, Environment, and Management (HNICEM ). IEEE. <https://doi.org/10.1109/hnicem48295.2019.9072751> (accessed Mar. 13, 2024).
- [15] Khadir, S., Andr n, D., Verre, R., Song, Q., Monneret, S., Genevet, P., K ll, M., & Baffou, G. (2021). Metasurface Optical Characterization Using Quadriwave Lateral Shearing Interferometry. *ACS Photonics*, 8(2), 603–613. <https://doi.org/10.1021/acsp Photonics.0c01707> (accessed Mar. 13, 2024).
- [16] Baffou, G. (2021). Quantitative phase microscopy using quadriwave lateral shearing interferometry (QLSI): principle, terminology, algorithm and grating shadow description. *Journal of Physics D: Applied Physics*, 54(29), 294002. (accessed Mar. 13, 2024).
- [17] Optical Interferometry. (n.d.). Retrieved March 13, 2024, from [http://physics.wm.edu/~evmik/classes/manual\\_for\\_Experimental\\_Atomic\\_Physics/interferometry\\_new.pdf](http://physics.wm.edu/~evmik/classes/manual_for_Experimental_Atomic_Physics/interferometry_new.pdf) (accessed Mar. 13, 2024).
- [18] Velghe, S., Primot, J., Gu r neau, N., Ha dar, R., Demoustier, S., Cohen, M., & Wattellier, B. (2006, August). Advanced wave-front sensing by quadri-wave lateral shearing interferometry. In *Interferometry XIII: Techniques and Analysis* (Vol. 6292, pp. 117-129). SPIE. (accessed Mar. 13, 2024).
- [19] plc, R. (n.d.). Renishaw: Interferometry explained. Renishaw. <https://www.renishaw.com/en/interferometry-explained--7854> (accessed Mar. 13, 2024).
- [20] Boucher, W., Velghe, S., Benoit Wattellier, & Gatinel, D. (2008, September). Intraocular lens characterization using a quadric-wave lateral shearing interferometer wave front sensor. ResearchGate; Society of Photo-optical Instrumentation Engineers. [https://www.researchgate.net/publication/228489020\\_Intraocular\\_lens\\_characterization\\_using\\_a\\_quadric-wave\\_lateral\\_shearing\\_interferometer\\_wave\\_front\\_sensor](https://www.researchgate.net/publication/228489020_Intraocular_lens_characterization_using_a_quadric-wave_lateral_shearing_interferometer_wave_front_sensor)

